

# CONSTRUCTING ORTHOGONAL WAVELET BASES ON THE SPHERE

*Daniela Roşca (1) and Jean-Pierre Antoine (2)*

(1) Technical University of Cluj-Napoca  
Department of Mathematics  
str. Daicoviciu 15, RO-400020 Cluj-Napoca, Romania  
email: Daniela.Rosca@math.utcluj.ro

(2) Institut de Physique Théorique (FYMA)  
Université Catholique de Louvain (UCL)  
B - 1348 Louvain-la-Neuve, Belgium  
email: jean-pierre.antoine@uclouvain.be

## ABSTRACT

The stereographic projection determines a bijection between the two-sphere, minus the North Pole, and the tangent plane at the South Pole. This correspondence induces a unitary map between the corresponding  $L^2$  spaces. Using this map, any plane wavelet may be lifted to a wavelet on the sphere. In this work we quickly review some existing constructions of spherical wavelets, then we apply the new procedure to orthogonal compactly supported wavelet bases in the plane and we get continuous, locally supported orthogonal wavelet bases on the sphere. As an example, we perform a singularity detection, where the other constructions of spherical wavelet bases fail.

## 1. INTRODUCTION

Two-dimensional wavelets are by now a standard tool in image processing, under the two concurrent approaches, the Discrete Wavelet Transform (DWT), based on the concept of multiresolution analysis, and the Continuous Wavelet Transform (CWT). While the former usually leads to wavelet bases, the CWT has to be discretized for numerical implementation and produces in general only frames.

Nowadays, many situations yield data on *spherical* surfaces. For instance, in Earth and Space sciences (geography, geodesy, meteorology, astronomy, cosmology, etc), in crystallography (texture analysis of crystals), in medicine (some organs are regarded as sphere-like surfaces), or in computer graphics (modelling of closed surfaces as the graph of a function defined on the sphere). Thus there is a need for suitable techniques for analyzing such data. In the spherical case, the Fourier transform amounts to an expansion in spherical harmonics, whose support is the whole sphere. Fourier analysis on the sphere is thus global and cumbersome. A possible replacement is to adapt the wavelet transform (WT) to the sphere.

## 2. THE CWT ON THE TWO-SPHERE

A first approach is to extend the CWT to the two sphere  $\mathbb{S}^2 = \{\mathbf{x} \in \mathbb{R}^3, \|\mathbf{x}\| = 1\}$ . A complete solution was obtained by Vandergheynst and one of us [1, 2], by a group-theoretical method. As it is well-known in the planar case, the design of a CWT on a given manifold  $X$  starts by identifying the operations one wants to perform on the finite energy signals living on  $X$ , that is, functions in  $L^2(X, d\nu)$ , where  $\nu$  is a suitable measure on  $X$ . Next one realizes these operations by unitary operators on  $L^2(X, d\nu)$  and one looks for a possible group-theoretical derivation.

In the case of the two-sphere  $\mathbb{S}^2$ , the required transformations are of two types: (i) *motions*, which are realized

by rotations  $\rho \in \text{SO}(3)$ , and (ii) *dilations* of some sort by a scale factor  $a \in \mathbb{R}_+^*$ . The problem is how to define properly the dilation *on the sphere*  $\mathbb{S}^2$ . The solution proposed in [1, 2] consists in lifting onto the sphere, by inverse *stereographic projection*, the usual radial dilation in the tangent plane at the South Pole. More precisely, the Hilbert space of spherical signals is  $L^2(\mathbb{S}^2, d\mu)$ , where  $d\mu = \sin \theta d\theta d\varphi$ ,  $\theta \in [0, \pi]$  is the colatitude angle,  $\varphi \in [0, 2\pi]$  the longitude angle,  $\omega = (\theta, \varphi) \in \mathbb{S}^2$ . In that space, the desired operations are realized by unitary operators on  $L^2(\mathbb{S}^2)$ :

- rotation  $R_\rho : (R_\rho f)(\omega) = f(\rho^{-1}\omega)$ ,  $\rho \in \text{SO}(3)$ ,
- dilation  $D_a : (D_a f)(\omega) = \lambda(a, \theta)^{1/2} f(\omega_{1/a})$ ,  $a \in \mathbb{R}_+^*$ .

In these relations,  $\omega_a = (\theta_a, \varphi)$ ,  $\theta_a$  is defined by  $\cot \frac{\theta_a}{2} = a \cot \frac{\theta}{2}$  for  $a > 0$  and the normalization factor  $\lambda(a, \theta)^{1/2}$  is needed for compensating the noninvariance of the measure  $\mu$  under dilation. Then, given an admissible wavelet  $\psi$ , the *spherical CWT* of a signal  $f \in L^2(\mathbb{S}^2)$  is defined by

$$W_\psi f(\rho, a) = \int_{\mathbb{S}^2} [R_\rho D_a \psi](\omega) f(\omega) d\mu(\omega). \quad (1)$$

Here the wavelet  $\psi$  is admissible if it belongs to  $L^2(\mathbb{S}^2)$  and satisfies the condition

$$\int_{\mathbb{S}^2} \frac{\psi(\theta, \varphi)}{1 - \cos \theta} d\mu(\omega) = 0.$$

This transform may be inverted and one gets an exact *reconstruction formula*. For a detailed analysis of continuous 2-D wavelet transforms, we refer to the monograph [3].

Although this spherical CWT was originally obtained by a group-theoretical method, the construction may be short-circuited if one remarks that it is uniquely determined by the geometry, in the sense that it suffices to impose *conformal* behavior of the relevant maps. More precisely, the stereographic projection is the unique conformal diffeomorphism from the sphere to its tangent plane at the South Pole. Similarly, the stereographic dilation is the unique radial dilation on the sphere that is conformal [18]. Thus one gets the formula (1) directly, without the sophisticated group-theoretical calculation.

A byproduct of the analysis is a complete equivalence between the spherical CWT and the usual planar CWT in the tangent plane, in the sense that the stereographic projection induces a unitary map  $\pi : L^2(\mathbb{S}^2) \rightarrow L^2(\mathbb{R}^2)$ . This fact allows one to lift any planar 2-D wavelet, including directional ones, onto the sphere by inverse stereographic projection.

The spherical CWT (1) may be discretized and one obtains frames, either half-continuous (only the scale variable  $a$  is discretized) or fully discrete [2, 5]. The method is easy to

implement, it leaves a large freedom in choosing the wavelet  $\psi$ , it allows the use of directional wavelets, it preserves smoothness and it gives no distortion around poles, since all points of  $\mathbb{S}^2$  are equivalent under the action of the operator  $R_\rho$ . However, it is computationally intensive, especially in the fully discrete case.

There is an alternative that also leads to a half-continuous wavelet representation on  $\mathbb{S}^2$ . It consists in using the so-called *harmonic* dilation instead of the stereographic one. This dilation acts on the Fourier coefficients of a function  $f$ , that is, the numbers  $\widehat{f}_{\ell,m} := \langle Y_\ell^m, f \rangle_{\mathbb{S}^2}$ , where  $\{Y_\ell^m, \ell \in \mathbb{N}, m = -\ell, \dots, \ell\}$  is the orthonormal basis of spherical harmonics in  $L^2(\mathbb{S}^2)$ . The dilation  $d_a$  is defined by the relation

$$(\widehat{d_a f})_{\ell,m} := f_{a\ell,m}, \quad a > 0.$$

This technique, originally due to Holschneider [10] and Freedman-Windheuser [8], has recently been revived in the applications to astrophysics [19]. However, although this definition leads to a well-defined, uniquely invertible wavelet representation, with steerable wavelets and full rotation invariance, there is no proof so far that it yields a frame. Hence one may question the stability of the reconstruction process, since it is the lower frame bound that guarantees it.

As a matter of fact, no discretization scheme leading to a wavelet basis is known, and the method applies to band-limited functions only. This entails high redundancy and thus a higher computing cost, which is not suitable for large data sets. There is also the problem of finding an appropriate discretization grid which leads to good frames.

For all those reasons, one would prefer to try and build directly a DWT on the sphere.

### 3. THE DWT ON THE SPHERE

Many authors have designed methods for constructing discrete spherical wavelets. All of them have advantages and drawbacks. These may be characterized in terms of several properties which are desirable for *any* efficient wavelet analysis, planar or spherical.

- *Basis*: The redundancy of frames leads to nonunique expansions. Moreover, the existing constructions of spherical frames are sometimes computationally heavy and often applicable only to band-limited functions.

- *Orthogonality*: This method leads to orthogonal reconstruction matrices, whose inversion is trivial. Thus, orthogonal bases are good for compression, but this is not always sufficient: sparsity of reconstruction matrices is still needed in the case of large data sets.

- *Local support*: This is crucial when working with large data sets, since it yields sparse matrices. Also, it prevents spreading of “tails” during approximation.<sup>1</sup>

- *Continuity, smoothness*: These properties are always desirable in approximation, but not easily achieved.

Let us quote a few of those methods, with focus on those properties, without being exhaustive (a more comprehensive review, with all references may be found in [4]).

#### (1) The spherical DWT using spherical harmonics

<sup>1</sup> A wavelet has *local support* if it vanishes identically outside a small region. It is *localized* if it is negligible outside a small region, so that it may have (small, but nonzero) “tails” there. Since these tails may spread in the process of approximation of data and spoil their good localization properties, local support is definitely preferred (see the example in [16]).

Various constructions of discrete spherical wavelets using spherical harmonics may be found in the literature, leading to frames or bases. The advantages of this method is that it produces no distortion (since no pole has a privileged role) and that it preserves smoothness of the wavelets. However, the wavelets so obtained have in general a localized support, but not a local one, i.e., it covers the whole sphere. Since this implies full reconstruction matrices, the result is not suitable for large amount of data. Examples are the works of Potts *et al.* [11] or Freedman and Schreiner [9].

#### (2) The spherical DWT via polar coordinates

The polar coordinate map  $\rho : I = [0, \pi] \times [0, 2\pi] \rightarrow \mathbb{S}^2$  has the familiar form  $\rho : (\theta, \varphi) \mapsto (\cos \varphi \sin \theta, \sin \varphi \sin \theta, \cos \theta)$ . A problem here is *continuity*. Indeed a continuous function  $f$  defined on  $I$  remains continuous after mapping it onto  $\mathbb{S}^2$  if and only if  $f(\theta, 0) = f(\theta, 2\pi)$ , for all  $\theta \in [0, \pi]$ , and there exists two constants  $P_N, P_S$  such that  $f(0, \varphi) = P_N$  and  $f(\pi, \varphi) = P_S$ , for all  $\varphi \in [0, 2\pi]$ . Unfortunately, these continuity conditions are not always easily satisfied by wavelets on intervals.

The obvious advantage of this approach is that many data sets are given in polar coordinates and thus one does not need to perform additional interpolation when implementing. However, there are disadvantages. First, no known construction gives both continuity and local support. Next, there are distortions around the poles:  $\rho$  maps the whole segment  $\{(0, \varphi), \varphi \in [0, 2\pi]\}$  onto the North Pole, and the whole segment  $\{(\pi, \varphi), \varphi \in [0, 2\pi]\}$  onto the South Pole. Representative examples are papers by Dahlke *et al.* [6] or Weinreich [17].

#### (3) The spherical DWT via radial projection from a convex polyhedron

Let  $\Gamma$  be a convex polyhedron, with vertices on  $\mathbb{S}^2$ , triangular faces and the center of the sphere inside  $\Gamma$ . The idea of the method, due to one of us [12, 14, 15], is to obtain wavelets on  $\mathbb{S}^2$  first by moving planar wavelets to wavelets defined on the faces of  $\Gamma$  and then projecting these radially onto  $\mathbb{S}^2$ . The resulting wavelets are orthogonal with respect to a weighted scalar product on  $L^2(\mathbb{S}^2)$ . This method offers many advantages: no distortion around the poles, possible construction of continuous and locally supported stable wavelet bases, local support of the wavelets (leading to sparse matrices), easy implementation, possible extension to sphere-like surfaces (closed surfaces) [13]. As a disadvantage, we may note the lack of smoothness of the wavelets.

As a matter of fact, no construction so far has led to wavelet bases on the sphere which are *simultaneously* continuous (or smoother), orthogonal and locally supported, although any two of these three conditions may be met at the same time. This suggests to try another approach.

### 4. LIFTING THE DWT FROM THE PLANE TO THE SPHERE

The method we propose consists in lifting wavelets from the tangent plane to the sphere by inverse stereographic projection [16]. It yields simultaneously smoothness, orthogonality, local support, vanishing moments. The disadvantage is that it gives distortions around a pole. In addition, although it is theoretically applicable to the whole pointed sphere  $\hat{\mathbb{S}}^2$ , in practice it can be used only for data “away” from that pole. However, the pole can be taken anywhere on the sphere, for

instance, in a region where no data is given. To give an example, European climatologists routinely put the North Pole of their spherical grid in the middle of the Pacific Ocean.

Our sphere is

$$\mathbb{S}^2 = \{\zeta = (\zeta_1, \zeta_2, \zeta_3) \in \mathbb{R}^3, \zeta_1^2 + \zeta_2^2 + (\zeta_3 - 1)^2 = 1\},$$

where we have used the parametrization  $\zeta_1 = \cos \varphi \sin \theta$ ,  $\zeta_2 = \sin \varphi \sin \theta$ ,  $\zeta_3 = 1 + \cos \theta$ , for  $\theta \in (0, \pi]$ ,  $\varphi \in [0, 2\pi)$ . The pointed sphere is  $\dot{\mathbb{S}}^2 = \mathbb{S}^2 \setminus \{(0, 0, 2)\}$ .

Let now  $p: \dot{\mathbb{S}}^2 \rightarrow \mathbb{R}^2$  be the stereographic projection from the North Pole  $N(0, 0, 2)$  onto the tangent plane  $\zeta_3 = 0$  at the South Pole. The area elements  $d\mathbf{x}$  of  $\mathbb{R}^2$  and  $d\mu(\zeta)$  of  $\dot{\mathbb{S}}^2$  are related by  $d\mathbf{x} = v(\zeta)^2 d\mu(\zeta)$ , where the weight factor  $v: \dot{\mathbb{S}}^2 \rightarrow \mathbb{R}$  is defined as

$$v(\zeta) = \frac{2}{2 - \zeta_3} = \frac{2}{1 - \cos \theta}, \quad \zeta = (\zeta_1, \zeta_2, \zeta_3) \equiv (\theta, \varphi) \in \dot{\mathbb{S}}^2.$$

Notice that  $L^2(\dot{\mathbb{S}}^2) := L^2(\dot{\mathbb{S}}^2, d\mu(\zeta)) = L^2(\mathbb{S}^2)$ , since the set  $\{N\}$  is of measure zero. As mentioned in Section 2, the stereographic projection  $p$  induces a unitary map  $\pi: L^2(\dot{\mathbb{S}}^2) \rightarrow L^2(\mathbb{R}^2)$ , with inverse  $\pi^{-1}: L^2(\mathbb{R}^2) \rightarrow L^2(\dot{\mathbb{S}}^2)$  given by  $\pi^{-1}(F) = v \cdot (F \circ p)$ ,  $\forall F \in L^2(\mathbb{R}^2)$ . As a consequence, we have

$$\langle F, G \rangle_{L^2(\mathbb{R}^2)} = \langle v \cdot (F \circ p), v \cdot (G \circ p) \rangle_{L^2(\dot{\mathbb{S}}^2)}, \quad \forall F, G \in L^2(\mathbb{R}^2). \quad (2)$$

This equality allows us to construct orthogonal bases on  $L^2(\dot{\mathbb{S}}^2)$  starting from orthogonal bases in  $L^2(\mathbb{R}^2)$ . More precisely, we will use the fact that, if the functions  $F, G \in L^2(\mathbb{R}^2)$  are orthogonal, then the functions  $F^s = v \cdot (F \circ p)$  and  $G^s = v \cdot (G \circ p)$  will be orthogonal in  $L^2(\dot{\mathbb{S}}^2)$ . Thus, the construction of multiresolution analysis (MRA) and wavelet bases in  $L^2(\dot{\mathbb{S}}^2)$  is based on the equality (2).

The starting point is a MRA in  $L^2(\mathbb{R}^2)$  (for a thorough analysis of MRAs in 1-D and in 2-D, we refer to the monograph [7]). For simplicity, we consider 2-D tensor wavelets, that is, we take the tensor product of two 1-D MRAs, with scaling function  $\phi$ , mother wavelet  $\psi$ , and diagonal dilation matrix  $D = \text{diag}(2, 2)$ . Thus we get a 2-D MRA of  $L^2(\mathbb{R}^2)$ , i.e., an increasing sequence of closed subspaces  $V_j \subset L^2(\mathbb{R}^2)$  with  $\bigcap_{j \in \mathbb{Z}} V_j = \{0\}$  and  $\overline{\bigcup_{j \in \mathbb{Z}} V_j} = L^2(\mathbb{R}^2)$ , satisfying the following conditions:

- (1)  $f(\cdot) \in V_j \iff f(D \cdot) \in V_{j+1}$ ,
- (2) There exists a function  $\Phi \in L^2(\mathbb{R}^2)$  such that the set  $\{\Phi(\cdot - \mathbf{k}), \mathbf{k} \in \mathbb{Z}^2\}$  is an orthonormal basis of  $V_0$ .

In terms of the original 1-D MRA, the 2-D scaling function is  $\Phi(\mathbf{x}) = \phi(x)\phi(y)$  and for the 2-D MRA it generates, one has

$$\begin{aligned} V_{j+1} &= V_{j+1} \otimes V_{j+1} = (V_j \oplus W_j) \otimes (V_j \oplus W_j) \\ &= (V_j \otimes V_j) \oplus [(W_j \otimes V_j) \oplus (V_j \otimes W_j) \oplus (W_j \otimes W_j)] \\ &= V_j \oplus W_j. \end{aligned}$$

Thus  $W_j$  consists of three pieces, with the following orthonormal bases:

$$\begin{aligned} &\{\psi_{j,k_1}(x)\phi_{j,k_2}(y), (k_1, k_2) \in \mathbb{Z}^2\} \text{ o.n.b. in } W_j \otimes V_j, \\ &\{\phi_{j,k_1}(x)\psi_{j,k_2}(y), (k_1, k_2) \in \mathbb{Z}^2\} \text{ o.n.b. in } V_j \otimes W_j, \\ &\{\psi_{j,k_1}(x)\psi_{j,k_2}(y), (k_1, k_2) \in \mathbb{Z}^2\} \text{ o.n.b. in } W_j \otimes W_j. \end{aligned}$$

This leads us to define three wavelets

$$\begin{aligned} {}^h\Psi(x, y) &= \phi(x)\psi(y), \\ {}^v\Psi(x, y) &= \psi(x)\phi(y), \\ {}^d\Psi(x, y) &= \psi(x)\psi(y). \end{aligned}$$

Then,  $\{{}^\lambda\Psi_{j,\mathbf{k}}, \mathbf{k} = (k_1, k_2) \in \mathbb{Z}^2, \lambda = h, v, d\}$  is an orthonormal basis for  $W_j$  and  $\{{}^\lambda\Psi_{j,\mathbf{k}}, j \in \mathbb{Z}, \mathbf{k} \in \mathbb{Z}^2, \lambda = h, v, d\}$  is an orthonormal basis for  $\bigoplus_{j \in \mathbb{Z}} W_j = L^2(\mathbb{R}^2)$ . Here, for  $j \in \mathbb{Z}, \mathbf{k} = (k_1, k_2) \in \mathbb{Z}^2$  and for  $F \in L^2(\mathbb{R}^2)$ , the function  $F_{j,\mathbf{k}}$  is defined as

$$F_{j,\mathbf{k}}(x, y) = 2^j F(2^j x - k_1, 2^j y - k_2).$$

Now we can proceed and lift the MRA to the sphere. To every function  $F \in L^2(\mathbb{R}^2)$ , one may associate the function  $F^s \in L^2(\dot{\mathbb{S}}^2)$  as  $F^s = v \cdot (F \circ p)$ . In particular,

$$F_{j,\mathbf{k}}^s = v \cdot (F_{j,\mathbf{k}} \circ p) \text{ for } j \in \mathbb{Z}, \mathbf{k} \in \mathbb{Z}^2, \quad (3)$$

and similarly for the spherical functions  $\Phi_{j,\mathbf{k}}^s$  and  ${}^\lambda\Psi_{j,\mathbf{k}}^s$ , where  $\Phi_{j,\mathbf{k}}, {}^\lambda\Psi_{j,\mathbf{k}}, \lambda = h, v, d$ , are the plane 2-D scaling functions and wavelets, respectively. For  $j \in \mathbb{Z}$ , we define  $\mathcal{V}_j$  as  $\mathcal{V}_j := \{v \cdot (F \circ p), F \in V_j\}$ . Then we have:

- (1)  $\mathcal{V}_j \subset \mathcal{V}_{j+1}$  for  $j \in \mathbb{Z}$ , and each  $\mathcal{V}_j$  is a closed subspace of  $L^2(\dot{\mathbb{S}}^2)$ ;
- (2)  $\bigcap_{j \in \mathbb{Z}} \mathcal{V}_j = \{0\}$  and  $\bigcup_{j \in \mathbb{Z}} \mathcal{V}_j$  is dense in  $L^2(\dot{\mathbb{S}}^2)$ ;
- (3)  $\{\Phi_{0,\mathbf{k}}^s, \mathbf{k} \in \mathbb{Z}^2\}$  is an orthonormal basis for  $\mathcal{V}_0$ .

A sequence  $(\mathcal{V}_j)_{j \in \mathbb{Z}}$  of subspaces of  $L^2(\dot{\mathbb{S}}^2)$  satisfying (1), (2), (3) constitutes a MRA of  $L^2(\dot{\mathbb{S}}^2)$ .

Define now the wavelet spaces  $\mathcal{W}_j$  by  $\mathcal{V}_{j+1} = \mathcal{V}_j \oplus \mathcal{W}_j$ . Then  $\{{}^\lambda\Psi_{j,\mathbf{k}}^s, \mathbf{k} \in \mathbb{Z}^2, \lambda = h, v, d\}$  is an orthonormal basis for  $\mathcal{W}_j$  and  $\{{}^\lambda\Psi_{j,\mathbf{k}}^s, j \in \mathbb{Z}, \mathbf{k} \in \mathbb{Z}^2, \lambda = h, v, d\}$  is an orthonormal basis for  $\overline{(\bigoplus_{j \in \mathbb{Z}} \mathcal{W}_j)} = L^2(\dot{\mathbb{S}}^2)$ .

In conclusion, if  $\Phi$  has compact support in  $\mathbb{R}^2$ , then  $\Phi_{j,\mathbf{k}}^s$  has local support on  $\mathbb{S}^2$  (and  $\text{diam supp } \Phi_{j,\mathbf{k}}^s \rightarrow 0$  as  $j \rightarrow \infty$ ), and similarly for the respective wavelets. An orthonormal 2-D wavelet basis yields an orthonormal spherical wavelet basis. Smooth 2-D wavelets yield smooth spherical wavelets. In particular, Daubechies wavelets yield locally supported and orthonormal wavelets on  $\dot{\mathbb{S}}^2$ . Thus the same tools as in the planar 2-D case can be used for the decomposition and reconstruction matrices (so that existing toolboxes may be used).

## 5. AN EXAMPLE: SINGULARITY DETECTION

As an application of our construction, we analyze the following zonal function on  $\mathbb{S}^2$ :

$$f(\theta, \varphi) = \begin{cases} 1, & \theta \leq \frac{\pi}{2}, \\ (1 + 3 \cos^2 \theta)^{-1/2}, & \theta \geq \frac{\pi}{2}. \end{cases} \quad (4)$$

The function  $f$  and its gradient are continuous, but the second partial derivative with respect to  $\theta$  has a discontinuity on the equator  $\theta = \frac{\pi}{2}$ . The function  $f$  is shown in Figure 1 (a). Detecting properly such a discontinuity requires a wavelet with three vanishing moments at least, so that, as far as we

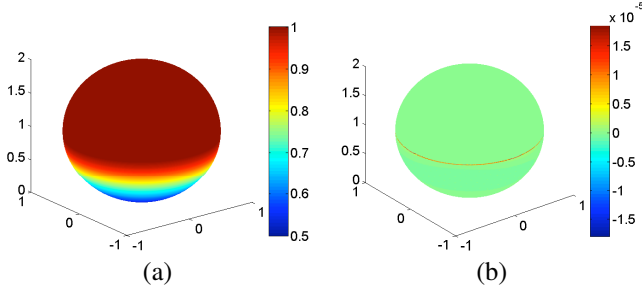


Figure 1: (a) The graph of the function  $f(\theta, \varphi)$  defined in (4); (b) Its analysis with the spherical wavelet associated to the familiar 6-coefficient Daubechies wavelet db3.

know, none of the existing constructions of discrete spherical wavelets could detect this discontinuity.

Instead, we consider the discretized spherical CWT with the spherical wavelet  $\Psi_{H_2}^s$  associated to the planar wavelet

$$\begin{aligned} \Psi_{H_2}(x, y) &= \Delta^2 [e^{-\frac{1}{2}(x^2+y^2)}] \\ &= (x^4 + y^4 + 2x^2y^2 - 8(x^2 + y^2) + 8)e^{-\frac{1}{2}(x^2+y^2)}. \end{aligned} \quad (5)$$

This wavelet has four vanishing moments (again a planar wavelet with less than three vanishing moments could not detect this discontinuity). The analysis is presented in Figure 2. Panels (a), (b), (c) and (d) present the spherical CWT at smaller and smaller scales,  $a = 0.08, 0.04, 0.02$  and  $0.0165$ , respectively. From Panels (a)-(c), it appears that the discontinuity along the equator is detected properly, and the precision increases as the scale decreases. However, there is a limit: when the scale  $a$  is taken below  $a = 0.018$ , the singularity is no more detected properly, and the transform is nonzero on the upper hemisphere, whereas the signal is constant there. This is visible on Panel (d), which shows the transform at scale  $a = 0.0165$ . In fact, the wavelet becomes too narrow and “falls in between” the discretization points, ripples appear in the Southern hemisphere. This effect is described in detail in [2].

On the contrary, the well-known Daubechies wavelet db3 lifted on the sphere by (3) does the job better than the wavelet  $\Psi_{H_2}^s$  mentioned above, as one can see in Figure 1, Panel (b). The computational load is smaller and the precision is much better, in the sense that the width of the detected singular curve is narrower.

The same tests were performed for the function  $f_{\pi/7}$ , obtained from  $f$  by performing a rotation around the axis  $Ox$  with an angle of  $\pi/7$ , in order to test the possible distortions in latitude when approaching the North Pole. The results are presented in Figure 3. Panel (a) shows the analysis of the function  $f_{\pi/7}$  with the discretized CWT method, using the wavelet  $\Psi_{H_2}^s$ , at scale  $a = 0.0165$ . Panel (b) gives the analysis with the Daubechies wavelet db3 lifted onto the sphere. No appreciable distortion is seen, the detection is good all along the discontinuity circle, and again the precision is better with the lifted Daubechies wavelet. Notice that the computation leading to the figure of Panel (a) was made with a grid finer than that used in Figure 2, so that the detection breaks down at a smaller scale (here below  $a = 0.01$ ).

Of course, this example is still academic, but it is significant. More work is needed, in particular, for estimating the

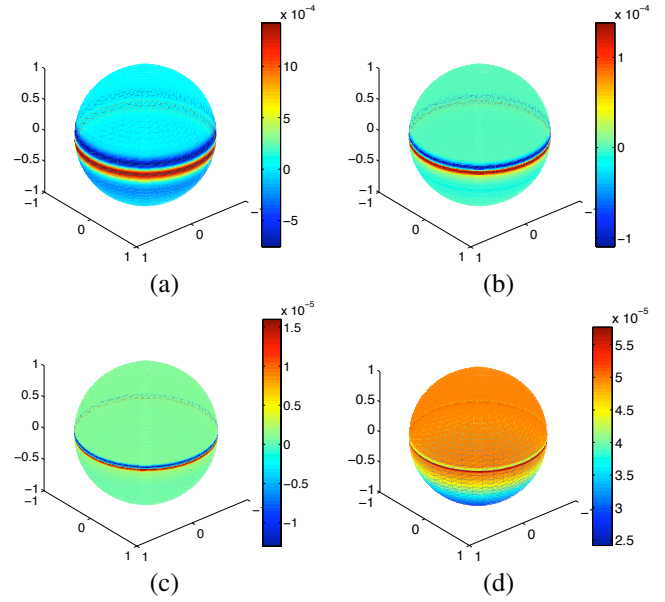


Figure 2: Analysis of the function  $f(\theta, \varphi)$  by the discretized CWT method with the wavelet  $\Psi_{H_2}^s$ , at scales: (a)  $a = 0.08$  (b)  $a = 0.04$  (c)  $a = 0.02$  (d)  $a = 0.0165$ . The sampling grid is  $256 \times 256$ .

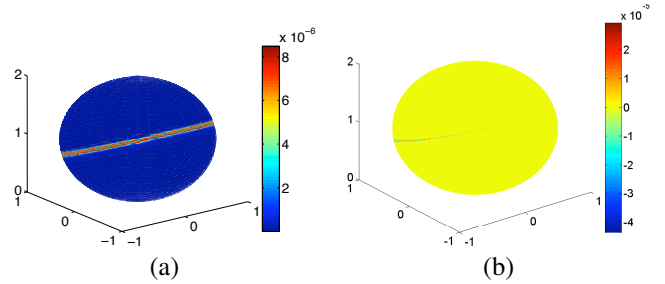


Figure 3: (a) Analysis of the function  $f_{\pi/7}(\theta, \varphi)$  by the discretized CWT method with the wavelet  $\Psi_{H_2}^s$ , at scale  $a = 0.0165$  (the sampling grid here is  $512 \times 512$ ); (b) Analysis of the function  $f_{\pi/7}(\theta, \varphi)$ , with the spherical wavelet associated to db3.

degree of distortion around the pole and applying the method to real life signals.

## ACKNOWLEDGEMENTS

We thank the anonymous referees for some constructive remarks.

## REFERENCES

- [1] J-P. Antoine and P. Vandergheynst, "Wavelets on the 2-sphere: A group-theoretical approach," *Applied Comput. Harmon. Anal.*, vol. 7, pp. 262–291, 1999.
- [2] J-P. Antoine, L. Demanet, L. Jacques, and P. Vandergheynst, "Wavelets on the sphere: Implementation and approximations," *Applied Comput. Harmon. Anal.*, vol. 13, pp. 177–200, 2002.
- [3] J-P. Antoine, R. Murenzi, P. Vandergheynst, and S.T. Ali, *Two-dimensional Wavelets and Their Relatives*. Cambridge University Press, Cambridge (UK), 2004.
- [4] J-P. Antoine and D. Roşca, "The wavelet transform on the two-sphere and related manifolds — A review," *Optical and Digital Image Processing*, Proc. SPIE, vol. 7000, 2008 (to appear).
- [5] I. Bogdanova, P. Vandergheynst, J-P. Antoine, L. Jacques, and M. Morvidone, "Stereographic wavelet frames on the sphere," *Appl. Comput. Harmon. Anal.*, vol. 26, pp. 223–252, 2005.
- [6] S. Dahlke, W. Dahmen, E. Schmidt, and I. Weinreich, "Multiresolution analysis and wavelets on  $\mathbb{S}^2$  and  $\mathbb{S}^3$ ," *Numer. Funct. Anal. Optim.*, vol. 16, pp. 19–41, 1995.
- [7] I. Daubechies, *Ten Lectures on Wavelets*. SIAM, Philadelphia, PA, 1992.
- [8] W. Freeden and U. Windheuser, "Combined spherical harmonic and wavelet expansion — A future concept in Earth's gravitational determination," *Applied Comput. Harmon. Anal.*, vol. 4, pp. 1–37, 1997.
- [9] W. Freeden and M. Schreiner, "Biorthogonal locally supported wavelets on the sphere based on zonal kernel functions," *J. Fourier Anal. Appl.*, vol. 13, pp. 693–709, 2007.
- [10] M. Holschneider, Continuous wavelet transforms on the sphere, *J. Math. Phys.* vol. 37, pp. 4156–4165, 1996.
- [11] D. Potts, G. Steidl, and M. Tasche, "Kernels of spherical harmonics and spherical frames", in *Advanced Topics in Multivariate Approximation*, F. Fontanella, K. Jetter and P.J. Laurent (eds.), World Scientific, Singapore, 1996, pp. 287–301.
- [12] D. Roşca, "Locally supported rational spline wavelets on the sphere," *Math. Comput.*, vol. 74 (252), pp. 1803–1829, 2005.
- [13] D. Roşca, "Piecewise constant wavelets defined on closed surfaces," *J. Comput. Anal. Appl.*, vol. 8(2), pp.121–132, 2006.
- [14] D. Roşca, "Weighted Haar wavelets on the sphere," *Int. J. Wavelets, Multires. and Inform. Proc.*, vol. 5 (3), pp. 501–511, 2007.
- [15] D. Roşca, "Wavelet bases on the sphere obtained by radial projection," *J. Fourier Anal. Appl.*, vol. 13, (4), pp. 421–434.
- [16] D. Roşca and J-P. Antoine, "Locally supported orthogonal wavelet bases on the sphere", preprint (submitted).
- [17] I. Weinreich, "A construction of  $C^1$ -wavelets on the two-dimensional sphere," *Applied Comput. Harmon. Anal.* vol. 10, pp. 1–26, 2001.
- [18] Y. Wiaux, L. Jacques, and P. Vandergheynst, "Correspondence principle between spherical and Euclidean wavelets," *Astrophys. J.*, vol. 632, pp. 15–28, 2005.
- [19] Y. Wiaux, J.D. McEwen, P. Vandergheynst, and O. Blanc, "Exact reconstruction with directional wavelets on the sphere," *Mon. Not. R. Astron. Soc.*, 2008 (in press); arXiv:0712.3519v2 [astro-ph].